New Findings Related to Carbothermal Reduction of Polysiloxane-derived Ceramics

Harrison Chaney, Kathy Lu*

Department of Materials Science and Engineering, Virginia Polytechnic Institute and State University, Blacksburg, Virginia 24061, USA

*Corresponding author: klu@vt.edu

Abstract:

Carbothermal reduction is the primary mechanism for SiC formation in polymer derived ceramics. However, the specific process involved in the SiOC conversion to SiC and the role of oxygen and carbon are unknown. Using ReaxFF with LAMMPS in a large simulation system containing more than 93K atoms, this study for the first time shows that O must be removed from SiO_2 clusters for SiC formation, providing insights into the carbothermal reduction mechanism. SiO_2 regions need to be of a large enough size to induce O reduction. C cluster growth is inversely related to removal of O. This work shows not only the importance of the simulation system size in understanding atomic interactions but also absence of phase separation of SiOC to SiO_2. Instead, SiO_2 converts to SiC through C diffusion and O removal.

Keywords: Carbothermal reduction; Polymer derived ceramics; ReaxFF; Oxygen removal; Cluster size

1. Introduction

Pyrolysis of polymer derived ceramics has been actively studied in recent years [1, 2]. Use of polysiloxane (PSO) as a preceramic precursor is of particular interest due to its highly tunable microstructure and the ability to create near net shapes in the pyrolysis stage [3]. Experimentally these precursors are pyrolyzed in a wide range of temperatures. The majority of mass loss occurs between 400 and 600°C through polymer decomposition [4]. At temperatures lower than 1300°C, there is no distinct crystalline regions [5]. Amorphous SiOC domains coexist with free C networks. At temperatures of greater than 1300°C, there is a notable decrease in O composition paired with the formation of β-SiC [6-8]. It is assumed that SiO_2 and free C react and O leaves the system as

CO [6, 7]. This is the well-accepted carbothermal reduction of Si-O bonds by C and formation of SiC through Si-C bonds.

Carbothermal reduction is characterized by two aspects. The reduction of O and the formation of β-SiC. There have been many theorized reaction routes that lead to the reduction of O. Eqs. (1) and (2) are two commonly theorized reactions [7]. Eq. (1) forms a SiO gas intermediate and Eq. (2) creates an amorphous Si intermediate.

$$C(s) + SiO_2(s) = SiO(g) + CO(g) \quad (1)$$

$$C(s) + SiO(g) = Si(s,l,g) + CO(g) \quad (2)$$

For the above reactions, there are two corresponding SiC formation reactions [7]:

$$2\,C(s) + SiO(g) = SiC(s) + CO(g) \quad (3)$$

$$Si(s,l,g) + C(s) = SiC(s) \quad (4)$$

Both of these theorized reactions play a role in the overall carbothermal reduction. For polymer derived ceramics, carbothermal reduction is commonly observed at pyrolysis temperatures higher than 1300°C and increases with temperature [6, 8, 9] [10]. In addition, SiO_2 clusters in such systems are resistant to phase transformation and remain small (<5 nm) and amorphous [11-14].

From a simulation perspective, there have not been many papers studying the pyrolysis of polymer derived ceramic systems. Of the limited papers published, molecular dynamic simulations demonstrate the formation of amorphous ceramic regions that cannot be seen experimentally. A hydridopolycarbosilane (HPCS) polymer was heated to 5000 K to simulate the polymer decomposition [15]. It was found that the C-H and Si-H bonds began to break at ~1000 K while the Si-C cleavage was not initiated until 2000 K. The pyrolysis of polydimethylsiloxane (PDMS) in the presence of water, NO, and ozone happened at 2500 K [16]. For a blend of HCPS and polyhydromethylsiloxane (PHMS) [17], Si-H, C-H, and Si-CH_3 bonds were broken at 1000 K while C-C bond formation increased at 1800 K. In addition, a new force field parameter was applied to the simulations of PHMS/HCPS [18]. When the temperature increased to 2500 K, which met the before-mentioned threshold of accelerated Si-C bond breakage, the simulation was able to illustrate phase separation and achieve experimentally verifiable end compositions [18].

However, none have been able to observe the fate of oxygen, which was one of the key aspects of carbothermal reduction discussed above. Among different factors, the small number of atoms used in the simulation systems is a major issue [19]. Previous studies used systems containing less than 10,000 atoms. Such small systems cannot sufficiently represent different domains and interactions in SiOC systems. They also limit the scalability of the results. Along this line, elevated temperatures and pressures [17, 18, 20] have been used to speed up pyrolysis kinetics and allow for relevant observations. However, such approaches inevitably alter the thermodynamics of bond breaking/formation and atomic diffusion.

This paper aims to address the system size deficiency in SiOC pyrolysis simulation by using ~100,000 atoms while achieving the simulation duration to ~6 ns. We demonstrate for the first time the removal of O through carbon diffusion, the first step in carbothermal reduction. In addition, different O loss behaviors are observed in different SiO_2 clusters. We have also explored the effects of O content on C cluster growth.

2. Computational Methods

A polysiloxane (PSO) precursor with a linear structure and random distribution of various hydrocarbon side groups was first created using Python. Eight of these linear polymer units, each having 100 Si-O backbone units, were spatially randomized. The overall system was consolidated using LAMMPS [21], a massively parallel molecular dynamic simulation software in conjunction with the ReaxFF potential package created by Van Duin et al [22, 23]. The consolidation simulation occurred over 200,000 timesteps under an isostatic pressure of 2 atm and a temperature of 300 K. A NPT thermostat was used for this step. At this stage the overall system had 11,070 atoms. The system was further expanded to 93,680 atoms by juxtaposing the initial simulation boxes.

The fully expanded system was heated gradually to 2,400 K in a two-step process. Each of the steps utilized a NPT system with an isostatic pressure of 2,000 atm. The timestep was also kept constant at 0.2 fs. The first heating phase took place in 0.2 ns and the system was heated from 300 K to 2,000 K. The second heating phase took place more gradually over the course of 0.4 ns from 2,000 K to 2,400 K. Gas species that were under 40 g/mol were deleted. After the temperature reached 2,400 K, the gas removal threshold was increased to 80 g/mol. This gas deletion regime was maintained for the rest of the simulation.

After the system reached 2,400 K, it was held at a constant pressure of 2,000 atm for 2.32 ns. During this time significant O was deleted as a gas byproduct. To ensure that the system reached equilibrium, the system was further heated to 2,600 K over the course of 0.38 ns and was allowed to hold at this temperature for additional 2.67 ns. The gas data were extracted using "fix reaxff/bonds" command with an upper bond limit set at 5 per atom. Table 1 shows the simulation condition comparisons with earlier studies.

Table 1. Comparison of atom number, temperature, and holding time in this and other studies.

Starting Polymer	Number of atoms	Holding Temperature (K)	Holding time at peak temperature (ns)	Source
PSO	93680	2400 2600	2.32 at 2400 K, 2.67 at 2600 K	This work
Polymethylhydridosiloxane, hydridopolycarbosilane	1628	1800	4.7	[17]
Polymethylhydridosiloxane, divinylbenzene	6144	2500	1	[18]

3. Results and Discussion

Fig. 1 shows the atomic structure and composition changes during the pyrolysis of PSO. Even though the H content seems high in atomic percent, the final H content is only ~1 wt%. In the initial SiOC system at 0 ns and 300 K, the atomic distributions of C, O, Si, and H reflect that of a crosslinked polymer structure (Fig. 1a). These species mix homogeneously throughout the system with no observable features. With the increase in pyrolysis time to 0.5 ns, both large and small SiO_2 clusters form as shown in Fig. 1b. Some Si-O rich clusters become connected, surrounded by a continuous carbon matrix. With the continuation of the pyrolysis to 1 ns and until completion, a large SiO_2 cluster appears and continues to mature (Figs. 1c and 1d). There are some smaller SiO_2 clusters in the carbon matrix; however, their overall volume is much smaller. This is the first time that such atomic structure evolution is observed. Previous studies cannot identify such an event due to the small number of atoms involved in the simulation, which cannot accommodate the space needed for multiple clusters of different sizes. Despite having similar simulation setups and using the same atomic potentials, our larger simulation system (15-57 times larger) can simulate the evolution of different size SiO_2 clusters (Figs. 1b-d) and their distributions.

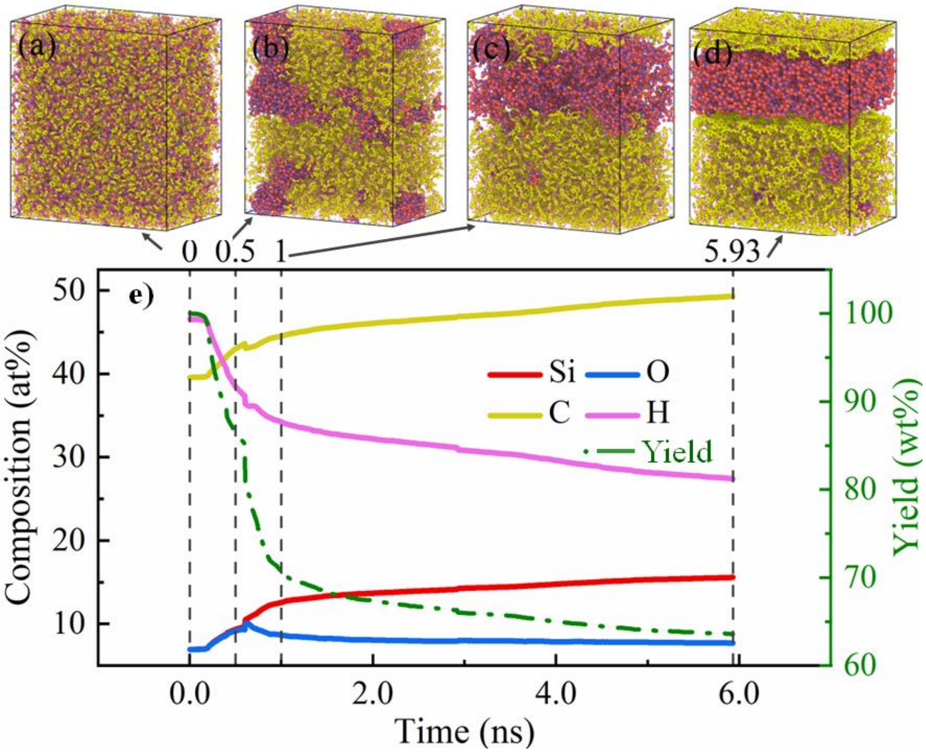

Fig. 1. SiOC atomic structure progression at 0 ns (a), 0.5 ns (b), 1 ns (c), and 6 ns (d). Composition changes with simulated pyrolysis time (e). In all the images, the color scheme is as follows: Si-red, O-blue, C-yellow, H-pink.

Fig. 1e shows the compositional changes with the simulation time. First, we observe that the O atomic percent increases from 6.9 to 10% and then decreases from 10% to 7.7%. Such O changes have not been simulated before even though it is a critical process for SiO_2 cluster carbothermal reduction. The increase is due to the release of C and H species and thus total decrease in number of atoms before loss in O. The decrease is due to the reduction in O from release of CO, O_2, and CO_2. Also, there is a Si and O content difference even though they have 1:1 ratio at the starting state. This difference has not been observed before. As surprisingly, there is a large difference in the compositions of the larger SiO_2 cluster and the smaller SiO_2 clusters. Most O loss occurs in the large SiO_2 cluster. The smaller SiO_2 clusters have little to no O loss and remain mostly unchanged throughout the simulation. The larger SiO_2 cluster has 29 at% O while the smaller SiO_2 clusters have 44 at% O at the end of the simulation. This implies that the O loss is sensitive to the size of the clusters. The larger SiO_2 region appears to be the main region capable of O reduction. This difference is directly related to the C diffusion discussed related to Fig. 3. Previous studies using smaller size simulation systems have not been able to capture this effect. This is further confirmed when comparing the O levels with previous simulations [18].

As shown in Fig. 1e, other compositional trends such as the increase in the Si atomic percent and the decrease in the H atomic percent have been observed in previous studies [17, 18]. Initially, most of the mass loss is attributed to losses in C and H due to polymer side group decomposition. The increases in C and Si coincide with the O loss while the decrease in H continues throughout the pyrolysis process. Because of the observed compositional differences over time, based on the size of the pyrolyzed SiOC system and the differences in the large and small SiO_2 clusters, the overall simulation system size is an important consideration for accurate description of the pyrolysis process.

The large O content difference in the large and small SiO_2 clusters indicates that the smaller SiO_2 regions are too small to absorb amorphous C. From fundamental point of view, this should be related to the lack of void space in the small SiO_2 clusters. In the traditional carbothermal reduction process, the smallest SiC particle size formed is >10 nm [24-26]. Some claims that the reaction SiC mechanism includes rapid formation of a gaseous SiO intermediate and reaction with

C [27]. In our study, the simulation temperature is much less than 1300°C in actual experimental systems [24-26, 28, 29]. Thus, SiO cannot be gasified. This new finding is also consistent with the widely observed resistance of SiO_2 cluster size increase in SiOC systems [6, 11-14, 30]. Most of the SiO_2 domains in SiOC remain at <5 nm size. This could be a residual result of carbothermal reduction of larger SiO_2 clusters and the carbothermal reduction resistance of the already reduced SiO_2 cluster cores below a threshold size. For the initially small SiO_2 clusters in this work, they remain small and stable throughout the pyrolysis process. Because of their small sizes, the atomic structures are also largely amorphous. When the SiO cluster size is <5 nm, SiC formed would be even smaller size. Many of such SiC clusters are unstable because of the small SiC size (less than the stable nuclei size). Thus, the carbothermal reduction process cannot proceed. This is an important finding and has only been observed in our simulation.

Fig. 2a shows the normalized Si-Si, Si-O, Si-C, and C-C bond changes over time. The Si-Si, Si-O, and Si-C bonds were normalized to the total number of Si-containing bonds and the C-C bond was normalized to the total number of C-containing bonds. There is a significant gain in Si-Si bonding as the simulation progresses, suggesting that Si-Si bonds act as an important intermediate in the reduction of O. This observation is consistent with the Si phase observed in earlier studies [30-32]. The gain in Si-Si bonds is mirrored by the loss in both Si-C and Si-O bonds. The initial loss in the Si-C bonds can be correlated with the hydrocarbon side group separation from the Si-O backbone and the amorphous C formation [33], as manifested by the C-C bond increase. The loss in the Si-C bonds is compensated by an increase in C atoms themselves. The Si-O bond loss, which lags the Si-C bond loss, is due to the C diffusion into the large Si-O rich cluster and replacing Si-O bonds with Si-C bonds (as shown in Figs. 3b and c).

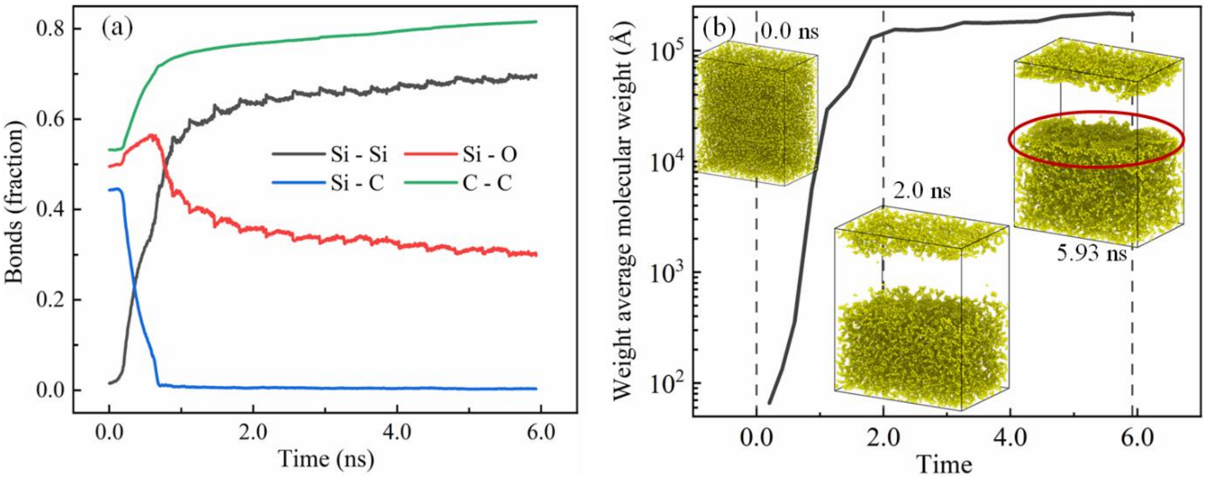

Fig. 2. Normalized Si-Si, Si-O, Si-C, and C-C bond changes over time (a), weight-averaged molecular weight of C along with C atomic distribution changes (b).

The weight-averaged molecular weight, which is used in polymers to determine the chain length, is shown in Fig. 2b for the C species to determine the C cluster size increase over time. The C cluster size increases exponentially from 0 to 2 ns and then plateaus for the remaining duration of the simulation. The drastic increase in the molecular weight indicates the bonding and growth of the C clusters as shown in the atomic structures. At the beginning of the pyrolysis, the C atoms form homogeneous and small clusters. At the beginning of the plateau region, there is segregation of C into discrete domains. More C atoms are bonded but still amorphous. At the end state of the plateau, separated C clusters continue to bond and grow into dense networks; there are clear graphitic regions at the Si-O rich cluster and C interface, as indicated by the red circle.

The decrease in Si-O bonds and thus the O deletion in Fig. 2a from 0.6 ns onwards coincide with the increase in the C cluster size as seen in Fig. 2b. In our earlier work [34, 35], we showed that for SiOC systems a higher C content leads higher electrical conductivity. Since the electrical conductivity for SiOC systems is through C, we can state that C cluster growth is correlated with less Si-O clusters and thus O removal. Other traditional SiO_2-C systems have shown that SiC growth increased with the C content by consuming SiO_2 [36]. In a conventional carbonaceous/SiO_2 hydrogel system, the dense glasses with a carbon content of <10 wt% are stable up to 1000°C in air. Heat treatment at 1300-1400° C renders porous structures and oxidation by air [25]. This again means that C growth leads to O removal. Earlier work suggested that carbothermal reduction is hindered by increased pressure [6]. In this study, the increased pressure used in simulations seems to result in faster C species growth and lower amounts of O reduction.

Fig. 3a shows the overall gas composition variations over time. The large peaks are the result of changes in the simulation conditions such as increases in temperature or in the molecular weight threshold. These peaks result from the discretization necessary for gas deletion in simulation. The important aspect to observe from Fig. 3a is the relative magnitude of different gas species. The rate of gas deletion after 2 ns remains very small for the rest of the simulation duration. As depicted in Fig. 3a, nearly all the changes in compositions are attributed to gas loss from H- and C-containing species before 0.6 ns. The deletion of O is not observed significantly until the system reaches a holding temperature of 2400 K. As noted previously, the larger SiO_2 cluster is the majority source of O loss. This is attributed to enabling the diffusion of larger C clusters by the larger SiO_2 cluster, which can only happen after the SiOC ceramic forms, not during the polymer decomposition. Figs. 3b and c show two consecutive images where large clusters of C are broken into smaller groups. This event occurs during the peak oxygen loss time span of 0.6 ns to 1ns and can be observed happening along the SiO_2-C interface. The size of C clusters plays an important role in the ability of C diffusing into the SiO_2 cluster and reacting with the O present. Larger C clusters must break apart to facilitate C diffusion into the Si-O network. This further confirms that only a sufficiently large SiO_2 domain can handle the diffusion of C clusters, as discussed earlier.

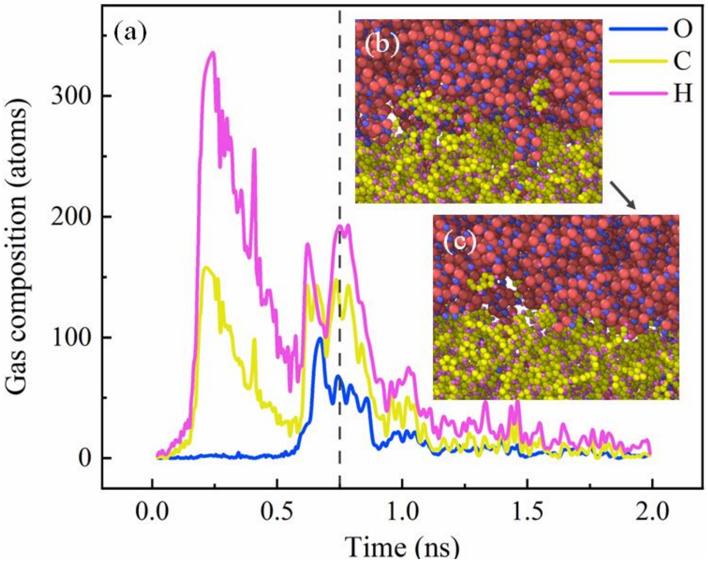

Fig. 3. (a) Gas loss over time; two consecutive atomic structures of a simulated region at 0.75 ns (b) and 0.7505 ns (c). In both images, the color scheme is as follows: Si-red, O-blue, C-yellow, H-pink.

4. Conclusions

In this work, carbothermal reduction of SiO_2 in PSO-derived SiOC ceramics was studied using ReaxFF simulation in LAMMPS with >93K atoms and up to ~6 ns simulation time. We demonstrate for the first time that SiOC evolves into different clusters during pyrolysis along with compositional changes, especially O loss. Also, SiO_2 cluster size plays an important role in the diffusion of C into SiO_2 clusters. Only larger SiO_2 clusters are capable of O reduction while smaller SiO_2 regions cannot accommodate C diffusion. C cluster growth is correlated with O removal. C diffusion into SiO_2 cluster further confirms that carbothermal reduction is dependent on SiO_2

cluster size. This is the first report on the O removal and C interaction with different SiO_2 clusters in polymer derived SiOC systems.

Author Contributions:

The manuscript was written through contributions of all authors. / All authors have given approval to the final version of the manuscript. / C. Chaney's contributions are conceptualization, data curation, formal analysis, investigation, methodology, software, validation, visualization, writing-original draft, writing-review & editing. K. Lu's contributions are conceptualization, formal analysis, funding acquisition, investigation, methodology, project administration, resources, supervision, validation, visualization, writing-original draft, writing-review & editing.

Funding Sources:

The authors would like to acknowledge the financial support from National Science Foundation under Grant No. CBET-2024546 and Air Force Office of Scientific Research under grant number FA9550-22-1-0081.

Competing Interests:

The authors declare that they have no known competing financial interests or non-financial interests that could have appeared to influence the work reported in this paper.

Data Availability:

The data required to reproduce these findings are available from https://data.lib.vt.edu.

References:

[1] N. Grassie, I.G. Macfarlane, K.F. Francey, The thermal degradation of polysiloxanes—II. Poly(methylphenylsiloxane), European Polymer Journal, 15 (1979) 415-422.

[2] N. Grassie, I.G. Macfarlane, The thermal degradation of polysiloxanes—I. Poly(dimethylsiloxane), European Polymer Journal, 14 (1978) 875-884.

[3] K. Lu, D. Erb, Polymer derived silicon oxycarbide-based coatings, International Materials Reviews, 63 (2018) 139-161.

[4] R. Ma, K. Lu, D. Erb, Effect of solvent in preparation of SiOC bulk ceramics, Materials Chemistry and Physics, 218 (2018) 140-146.

[5] D. Erb, K. Lu, Effect of additive structure and size on SiO_2 formation in polymer-derived SiOC ceramics, Journal of the American Ceramic Society, 101 (2018) 5378-5388.

[6] Q. Wen, Z. Yu, R. Riedel, The fate and role of in situ formed carbon in polymer-derived ceramics, Progress in Materials Science, 109 (2020) 100623.

[7] A.W. Weimer, K.J. Nilsen, G.A. Cochran, R.P. Roach, Kinetics of carbothermal reduction synthesis of beta silicon carbide, AIChE Journal, 39 (1993) 493-503.

[8] A.V. Rau, K. Knott, K. Lu, Porous SiOC/SiC ceramics via an active-filler-catalyzed polymer-derived method, Materials Chemistry Frontiers, 5 (2021) 6530-6545.

[9] L. Wang, K. Lu, R. Ma, Effects of different polymer precursors on the characteristics of SiOC bulk ceramics, Applied Physics A, 125 (2019).

[10] P. Colombo, G. Mera, R. Riedel, G.D. Sorarù, Polymer-derived ceramics: 40 years of research and innovation in advanced ceramics, Journal of the American Ceramic Society, (2010) 1805–1837.

[11] D. Erb, K. Lu, Effects of SiO_2-forming additive on polysiloxane derived SiOC ceramics, Microporous and Mesoporous Materials, 266 (2018) 75-82.

[12] D. Erb, K. Lu, Effect of additive structure and size on SiO_2 formation in polymer-derived SiOC ceramics, Journal of the American Ceramic Society, 101 (2018) 5378-5388.

[13] J.K. Li, K. Lu, T.S. Lin, F.Y. Shen, Preparation of micro-/mesoporous SiOC bulk ceramics, Journal of the American Ceramic Society, 98 (2015) 1753-1761.

[14] K. Lu, Porous and high surface area silicon oxycarbide-based materials-A review, Materials Science and Engineering R, 97 (2015) 23-49.

[15] S. Naserifar, L. Liu, W.A. Goddard, T.T. Tsotsis, M. Sahimi, Toward a process-based molecular model of SiC membranes. 1. Development of a Reactive Force Field, The Journal of Physical Chemistry C, 117 (2013) 3308-3319.

[16] K. Chenoweth, S. Cheung, A.C.T. Van Duin, W.A. Goddard, E.M. Kober, Simulations on the thermal decomposition of a poly(dimethylsiloxane) polymer using the ReaxFF Reactive Force Field, Journal of the American Chemical Society, 127 (2005) 7192-7202.

[17] H.F. Gao, H.J. Wang, Z.H. Zhao, M. Niu, L. Su, Y. Wei, Reactive dynamics simulation study on the pyrolysis of polymer precursors to generate amorphous silicon oxycarbide structures, Journal of Physical Chemistry C, 122 (2018) 5767-5773.

[18] I. Ponomarev, A.C.T. van Duin, P. Kroll, Reactive Force Field for simulations of the pyrolysis of polysiloxanes into silicon oxycarbide ceramics, The Journal of Physical Chemistry C, 123 (2019) 16804-16812.

[19] R. Montgomery-Walsh, S. Nimbalkar, J. Bunnell, S.L. Galindo, S. Kassegne, Molecular dynamics simulation of evolution of nanostructures and functional groups in glassy carbon under pyrolysis, Carbon, 184 (2021) 627-640.

[20] C. Ma, Y. Li, Phase transition in polymer derived ceramics (PDCs) and its effect on mechanical response, International Journal of Computational Materials Science and Engineering, 12 (2021) 1962-1972.

[21] A.P. Thompson, H.M. Aktulga, R. Berger, D.S. Bolintineanu, W.M. Brown, P.S. Crozier, P.J. in 't Veld, A. Kohlmeyer, S.G. Moore, T.D. Nguyen, R. Shan, M.J. Stevens, J. Tranchida, C. Trott, S.J. Plimpton, LAMMPS - a flexible simulation tool for particle-based materials modeling at the atomic, meso, and continuum scales, Computer Physics Communications, 271 (2022) 108171.

[22] A.C.T. van Duin, S. Dasgupta, F. Lorant, W.A. Goddard, ReaxFF: A Reactive Force Field for hydrocarbons, The Journal of Physical Chemistry A, 105 (2001) 9396-9409.

[23] H.M. Aktulga, J.C. Fogarty, S.A. Pandit, A.Y. Grama, Parallel reactive molecular dynamics: Numerical methods and algorithmic techniques, Parallel Computing, 38 (2012) 245-259.

[24] N. Keller, O. Reiff, V. Keller, M.J. Ledoux, High surface area submicrometer-sized beta-SiC particles grown by shape memory synthesis method, Diamond & Related Materials, 14 (2005) 1353-1360.

[25] H. Preiss, L.M. Berger, M. Braun, Formation of black glasses and silicon carbide from binary carbonaceous/silica hydrogels, Carbon, 33 (1995) 1739-1746.

[26] M. Sharma, R.K. Upadhyay, S.S. Amritphale, N. Chandra, Synthesis of nano-structured 3C-SiC by carbothermal reduction of silicon bearing gel and carbon soot, Materials Letters, 65 (2011) 2161-2164.

[27] A.W. Weimer, K.J. Nilsen, G.A. Cochran, R.P. Roach, Kinetics of carbothermal reduction synthesis of beta silicon-carbide, AIChE Journal, 39 (1993) 493-503.

[28] Y. Hwang, D.H. Riu, H.J. Kang, J.H. An, W.S. Jung, D. Chun, Y. Kim, Carbothermal synthesis of beta-SiC powders from silicon and SiO_2-coated carbon powders, International Journal of Materials Research, 105 (2014) 392-396.

[28] K. Wang, H.T. Wang, Y.B. Cheng, Synthesis of nanostructured silicon carbide spheres from mesoporous C-SiO_2 nanocomposites, Chemical Communications, 46 (2010) 303-305.

[30] J.K. Li, K. Lu, Highly porous SiOC bulk ceramics with water vapor assisted pyrolysis, Journal of the American Ceramic Society, 98 (2015) 2357-2365.

[31] J. Latournerie, P. Dempsey, D. Hourlier-Bahloul, J.-P. Bonnet, Silicon oxycarbide glasses: Part 1—Thermochemical stability, Journal of the American Ceramic Society, 89 (2006) 1485-1491.

[32] G. Gregori, H.-J. Kleebe, D.W. Readey, G.D. Sorarù, Energy-filtered TEM study of Ostwald ripening of Si nanocrystals in a SiOC glass, Journal of the American Ceramic Society, 89 (2006) 1699-1703.

[33] S. Yu, R. Tu, T. Goto, Preparation of SiOC nanocomposite films by laser chemical vapor deposition, Journal of the European Ceramic Society, 36 (2016) 403-409.

[34] L. Wang, K. Lu, R. Ma, Effects of different polymer precursors on the characteristics of SiOC bulk ceramics, Applied Physics A, 125 (2019) 395.

[35] L. Wang, K. Lu, Phase development of silicon oxycarbide nanocomposites during flash pyrolysis, Journal of Materials Science, 54 (2019) 6073-6087.

[36] S. Cetinkaya, S. Eroglu, Chemical vapor deposition of C on SiO_2 and subsequent carbothermal reduction for the synthesis of nanocrystalline SiC particles/whiskers, International Journal of Refractory Metals and Hard Materials, 29 (2011) 566-572.

New Findings Related to Carbothermal Reduction of Polysiloxane-derived Ceramics

Harrison Chaney, Kathy Lu*

Department of Materials Science and Engineering, Virginia Polytechnic Institute and State University, Blacksburg, Virginia 24061, USA

*Corresponding author: klu@vt.edu

Abstract:

Carbothermal reduction is the primary mechanism for SiC formation in polymer derived ceramics. However, the specific process involved in the SiOC conversion to SiC and the role of oxygen and carbon are unknown. Using ReaxFF with LAMMPS in a large simulation system containing more than 93K atoms, this study for the first time shows that O must be removed from SiO_2 clusters for SiC formation, providing insights into the carbothermal reduction mechanism. SiO_2 regions need to be of a large enough size to induce O reduction. C cluster growth is inversely related to removal of O. This work shows not only the importance of the simulation system size in understanding atomic interactions but also absence of phase separation of SiOC to SiO_2. Instead, SiO_2 converts to SiC through C diffusion and O removal.

Keywords: Carbothermal reduction; Polymer derived ceramics; ReaxFF; Oxygen removal; Cluster size

1. Introduction

Pyrolysis of polymer derived ceramics has been actively studied in recent years [1, 2]. Use of polysiloxane (PSO) as a preceramic precursor is of particular interest due to its highly tunable microstructure and the ability to create near net shapes in the pyrolysis stage [3]. Experimentally these precursors are pyrolyzed in a wide range of temperatures. The majority of mass loss occurs between 400 and 600°C through polymer decomposition [4]. At temperatures lower than 1300°C, there is no distinct crystalline regions [5]. Amorphous SiOC domains coexist with free C networks. At temperatures of greater than 1300°C, there is a notable decrease in O composition paired with the formation of β-SiC [6-8]. It is assumed that SiO_2 and free C react and O leaves the system as

CO [6, 7]. This is the well-accepted carbothermal reduction of Si-O bonds by C and formation of SiC through Si-C bonds.

Carbothermal reduction is characterized by two aspects. The reduction of O and the formation of β-SiC. There have been many theorized reaction routes that lead to the reduction of O. Eqs. (1) and (2) are two commonly theorized reactions [7]. Eq. (1) forms a SiO gas intermediate and Eq. (2) creates an amorphous Si intermediate.

$$C(s) + SiO_2(s) = SiO(g) + CO(g) \tag{1}$$

$$C(s) + SiO(g) = Si(s,l,g) + CO(g) \tag{2}$$

For the above reactions, there are two corresponding SiC formation reactions [7]:

$$2\,C(s) + SiO(g) = SiC(s) + CO(g) \tag{3}$$

$$Si(s,l,g) + C(s) = SiC(s) \tag{4}$$

Both of these theorized reactions play a role in the overall carbothermal reduction. For polymer derived ceramics, carbothermal reduction is commonly observed at pyrolysis temperatures higher than 1300°C and increases with temperature [6, 8, 9] [10]. In addition, SiO_2 clusters in such systems are resistant to phase transformation and remain small (<5 nm) and amorphous [11-14].

From a simulation perspective, there have not been many papers studying the pyrolysis of polymer derived ceramic systems. Of the limited papers published, molecular dynamic simulations demonstrate the formation of amorphous ceramic regions that cannot be seen experimentally. A hydridopolycarbosilane (HPCS) polymer was heated to 5000 K to simulate the polymer decomposition [15]. It was found that the C-H and Si-H bonds began to break at ~1000 K while the Si-C cleavage was not initiated until 2000 K. The pyrolysis of polydimethylsiloxane (PDMS) in the presence of water, NO, and ozone happened at 2500 K [16]. For a blend of HCPS and polyhydromethylsiloxane (PHMS) [17], Si-H, C-H, and Si-CH_3 bonds were broken at 1000 K while C-C bond formation increased at 1800 K. In addition, a new force field parameter was applied to the simulations of PHMS/HCPS [18]. When the temperature increased to 2500 K, which met the before-mentioned threshold of accelerated Si-C bond breakage, the simulation was able to illustrate phase separation and achieve experimentally verifiable end compositions [18].

However, none have been able to observe the fate of oxygen, which was one of the key aspects of carbothermal reduction discussed above. Among different factors, the small number of atoms used in the simulation systems is a major issue [19]. Previous studies used systems containing less than 10,000 atoms. Such small systems cannot sufficiently represent different domains and interactions in SiOC systems. They also limit the scalability of the results. Along this line, elevated temperatures and pressures [17, 18, 20] have been used to speed up pyrolysis kinetics and allow for relevant observations. However, such approaches inevitably alter the thermodynamics of bond breaking/formation and atomic diffusion.

This paper aims to address the system size deficiency in SiOC pyrolysis simulation by using ~100,000 atoms while achieving the simulation duration to ~6 ns. We demonstrate for the first time the removal of O through carbon diffusion, the first step in carbothermal reduction. In addition, different O loss behaviors are observed in different SiO_2 clusters. We have also explored the effects of O content on C cluster growth.

2. Computational Methods

A polysiloxane (PSO) precursor with a linear structure and random distribution of various hydrocarbon side groups was first created using Python. Eight of these linear polymer units, each having 100 Si-O backbone units, were spatially randomized. The overall system was consolidated using LAMMPS [21], a massively parallel molecular dynamic simulation software in conjunction with the ReaxFF potential package created by Van Duin et al [22, 23]. The consolidation simulation occurred over 200,000 timesteps under an isostatic pressure of 2 atm and a temperature of 300 K. A NPT thermostat was used for this step. At this stage the overall system had 11,070 atoms. The system was further expanded to 93,680 atoms by juxtaposing the initial simulation boxes.

The fully expanded system was heated gradually to 2,400 K in a two-step process. Each of the steps utilized a NPT system with an isostatic pressure of 2,000 atm. The timestep was also kept constant at 0.2 fs. The first heating phase took place in 0.2 ns and the system was heated from 300 K to 2,000 K. The second heating phase took place more gradually over the course of 0.4 ns from 2,000 K to 2,400 K. Gas species that were under 40 g/mol were deleted. After the temperature reached 2,400 K, the gas removal threshold was increased to 80 g/mol. This gas deletion regime was maintained for the rest of the simulation.

After the system reached 2,400 K, it was held at a constant pressure of 2,000 atm for 2.32 ns. During this time significant O was deleted as a gas byproduct. To ensure that the system reached equilibrium, the system was further heated to 2,600 K over the course of 0.38 ns and was allowed to hold at this temperature for additional 2.67 ns. The gas data were extracted using "fix reaxff/bonds" command with an upper bond limit set at 5 per atom. Table 1 shows the simulation condition comparisons with earlier studies.

Table 1. Comparison of atom number, temperature, and holding time in this and other studies.

Starting Polymer	Number of atoms	Holding Temperature (K)	Holding time at peak temperature (ns)	Source
PSO	93680	2400 2600	2.32 at 2400 K, 2.67 at 2600 K	This work
Polymethylhydridosiloxane, hydridopolycarbosilane	1628	1800	4.7	[17]
Polymethylhydridosiloxane, divinylbenzene	6144	2500	1	[18]

3. Results and Discussion

Fig. 1 shows the atomic structure and composition changes during the pyrolysis of PSO. Even though the H content seems high in atomic percent, the final H content is only ~1 wt%. In the initial SiOC system at 0 ns and 300 K, the atomic distributions of C, O, Si, and H reflect that of a crosslinked polymer structure (Fig. 1a). These species mix homogeneously throughout the system with no observable features. With the increase in pyrolysis time to 0.5 ns, both large and small SiO_2 clusters form as shown in Fig. 1b. Some Si-O rich clusters become connected, surrounded by a continuous carbon matrix. With the continuation of the pyrolysis to 1 ns and until completion, a large SiO_2 cluster appears and continues to mature (Figs. 1c and 1d). There are some smaller SiO_2 clusters in the carbon matrix; however, their overall volume is much smaller. This is the first time that such atomic structure evolution is observed. Previous studies cannot identify such an event due to the small number of atoms involved in the simulation, which cannot accommodate the space needed for multiple clusters of different sizes. Despite having similar simulation setups and using the same atomic potentials, our larger simulation system (15-57 times larger) can simulate the evolution of different size SiO_2 clusters (Figs. 1b-d) and their distributions.

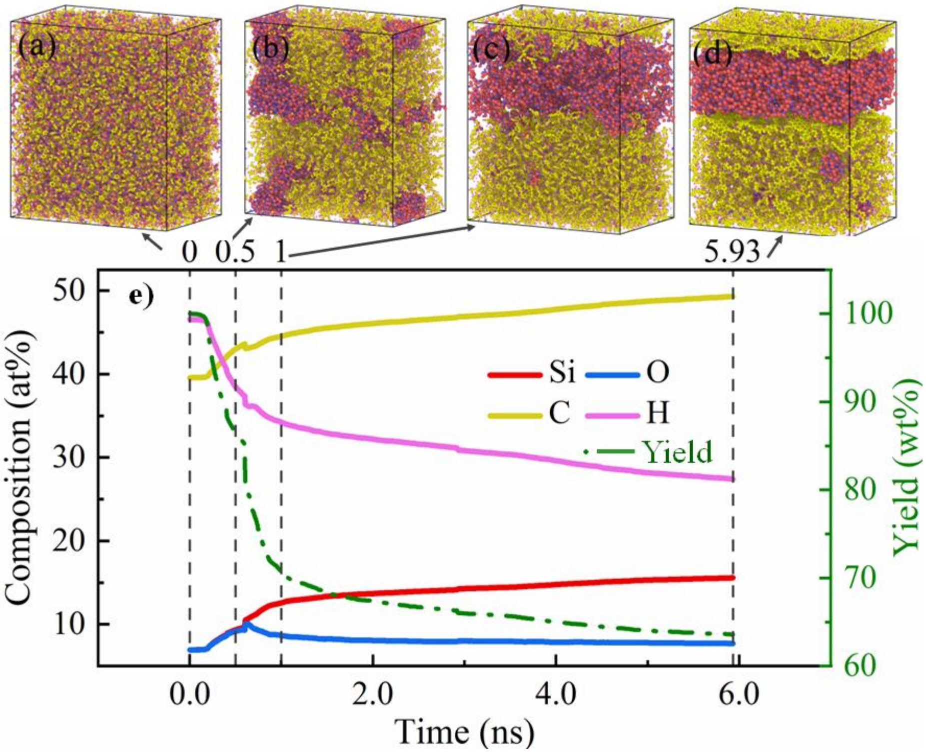

Fig. 1. SiOC atomic structure progression at 0 ns (a), 0.5 ns (b), 1 ns (c), and 6 ns (d). Composition changes with simulated pyrolysis time (e). In all the images, the color scheme is as follows: Si-red, O-blue, C-yellow, H-pink.

Fig. 1e shows the compositional changes with the simulation time. First, we observe that the O atomic percent increases from 6.9 to 10% and then decreases from 10% to 7.7%. Such O changes have not been simulated before even though it is a critical process for SiO_2 cluster carbothermal reduction. The increase is due to the release of C and H species and thus total decrease in number of atoms before loss in O. The decrease is due to the reduction in O from release of CO, O_2, and CO_2. Also, there is a Si and O content difference even though they have 1:1 ratio at the starting state. This difference has not been observed before. As surprisingly, there is a large difference in the compositions of the larger SiO_2 cluster and the smaller SiO_2 clusters. Most O loss occurs in the large SiO_2 cluster. The smaller SiO_2 clusters have little to no O loss and remain mostly unchanged throughout the simulation. The larger SiO_2 cluster has 29 at% O while the smaller SiO_2 clusters have 44 at% O at the end of the simulation. This implies that the O loss is sensitive to the size of the clusters. The larger SiO_2 region appears to be the main region capable of O reduction. This difference is directly related to the C diffusion discussed related to Fig. 3. Previous studies using smaller size simulation systems have not been able to capture this effect. This is further confirmed when comparing the O levels with previous simulations [18].

As shown in Fig. 1e, other compositional trends such as the increase in the Si atomic percent and the decrease in the H atomic percent have been observed in previous studies [17, 18]. Initially, most of the mass loss is attributed to losses in C and H due to polymer side group decomposition. The increases in C and Si coincide with the O loss while the decrease in H continues throughout the pyrolysis process. Because of the observed compositional differences over time, based on the size of the pyrolyzed SiOC system and the differences in the large and small SiO_2 clusters, the overall simulation system size is an important consideration for accurate description of the pyrolysis process.

The large O content difference in the large and small SiO_2 clusters indicates that the smaller SiO_2 regions are too small to absorb amorphous C. From fundamental point of view, this should be related to the lack of void space in the small SiO_2 clusters. In the traditional carbothermal reduction process, the smallest SiC particle size formed is >10 nm [24-26]. Some claims that the reaction SiC mechanism includes rapid formation of a gaseous SiO intermediate and reaction with

C [27]. In our study, the simulation temperature is much less than 1300°C in actual experimental systems [24-26, 28, 29]. Thus, SiO cannot be gasified. This new finding is also consistent with the widely observed resistance of SiO_2 cluster size increase in SiOC systems [6, 11-14, 30]. Most of the SiO_2 domains in SiOC remain at <5 nm size. This could be a residual result of carbothermal reduction of larger SiO_2 clusters and the carbothermal reduction resistance of the already reduced SiO_2 cluster cores below a threshold size. For the initially small SiO_2 clusters in this work, they remain small and stable throughout the pyrolysis process. Because of their small sizes, the atomic structures are also largely amorphous. When the SiO cluster size is <5 nm, SiC formed would be even smaller size. Many of such SiC clusters are unstable because of the small SiC size (less than the stable nuclei size). Thus, the carbothermal reduction process cannot proceed. This is an important finding and has only been observed in our simulation.

Fig. 2a shows the normalized Si-Si, Si-O, Si-C, and C-C bond changes over time. The Si-Si, Si-O, and Si-C bonds were normalized to the total number of Si-containing bonds and the C-C bond was normalized to the total number of C-containing bonds. There is a significant gain in Si-Si bonding as the simulation progresses, suggesting that Si-Si bonds act as an important intermediate in the reduction of O. This observation is consistent with the Si phase observed in earlier studies [30-32]. The gain in Si-Si bonds is mirrored by the loss in both Si-C and Si-O bonds. The initial loss in the Si-C bonds can be correlated with the hydrocarbon side group separation from the Si-O backbone and the amorphous C formation [33], as manifested by the C-C bond increase. The loss in the Si-C bonds is compensated by an increase in C atoms themselves. The Si-O bond loss, which lags the Si-C bond loss, is due to the C diffusion into the large Si-O rich cluster and replacing Si-O bonds with Si-C bonds (as shown in Figs. 3b and c).

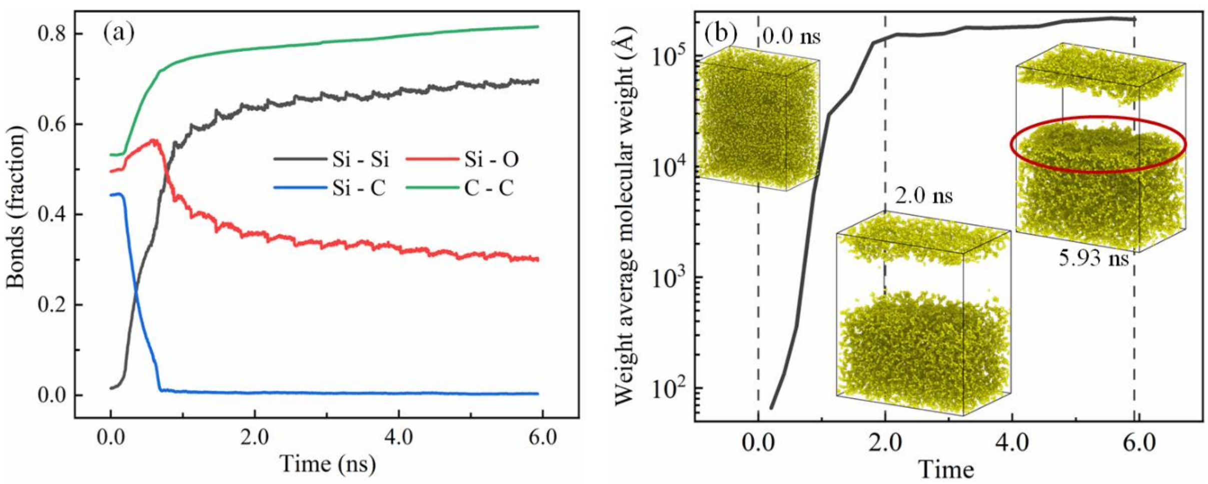

Fig. 2. Normalized Si-Si, Si-O, Si-C, and C-C bond changes over time (a), weight-averaged molecular weight of C along with C atomic distribution changes (b).

The weight-averaged molecular weight, which is used in polymers to determine the chain length, is shown in Fig. 2b for the C species to determine the C cluster size increase over time. The C cluster size increases exponentially from 0 to 2 ns and then plateaus for the remaining duration of the simulation. The drastic increase in the molecular weight indicates the bonding and growth of the C clusters as shown in the atomic structures. At the beginning of the pyrolysis, the C atoms form homogeneous and small clusters. At the beginning of the plateau region, there is segregation of C into discrete domains. More C atoms are bonded but still amorphous. At the end state of the plateau, separated C clusters continue to bond and grow into dense networks; there are clear graphitic regions at the Si-O rich cluster and C interface, as indicated by the red circle.

The decrease in Si-O bonds and thus the O deletion in Fig. 2a from 0.6 ns onwards coincide with the increase in the C cluster size as seen in Fig. 2b. In our earlier work [34, 35], we showed that for SiOC systems a higher C content leads higher electrical conductivity. Since the electrical conductivity for SiOC systems is through C, we can state that C cluster growth is correlated with less Si-O clusters and thus O removal. Other traditional SiO_2-C systems have shown that SiC growth increased with the C content by consuming SiO_2 [36]. In a conventional carbonaceous/SiO_2 hydrogel system, the dense glasses with a carbon content of <10 wt% are stable up to 1000°C in air. Heat treatment at 1300-1400° C renders porous structures and oxidation by air [25]. This again means that C growth leads to O removal. Earlier work suggested that carbothermal reduction is hindered by increased pressure [6]. In this study, the increased pressure used in simulations seems to result in faster C species growth and lower amounts of O reduction.

Fig. 3a shows the overall gas composition variations over time. The large peaks are the result of changes in the simulation conditions such as increases in temperature or in the molecular weight threshold. These peaks result from the discretization necessary for gas deletion in simulation. The important aspect to observe from Fig. 3a is the relative magnitude of different gas species. The rate of gas deletion after 2 ns remains very small for the rest of the simulation duration. As depicted in Fig. 3a, nearly all the changes in compositions are attributed to gas loss from H- and C-containing species before 0.6 ns. The deletion of O is not observed significantly until the system reaches a holding temperature of 2400 K. As noted previously, the larger SiO_2 cluster is the majority source of O loss. This is attributed to enabling the diffusion of larger C clusters by the larger SiO_2 cluster, which can only happen after the SiOC ceramic forms, not during the polymer decomposition. Figs. 3b and c show two consecutive images where large clusters of C are broken into smaller groups. This event occurs during the peak oxygen loss time span of 0.6 ns to 1ns and can be observed happening along the SiO_2-C interface. The size of C clusters plays an important role in the ability of C diffusing into the SiO_2 cluster and reacting with the O present. Larger C clusters must break apart to facilitate C diffusion into the Si-O network. This further confirms that only a sufficiently large SiO_2 domain can handle the diffusion of C clusters, as discussed earlier.

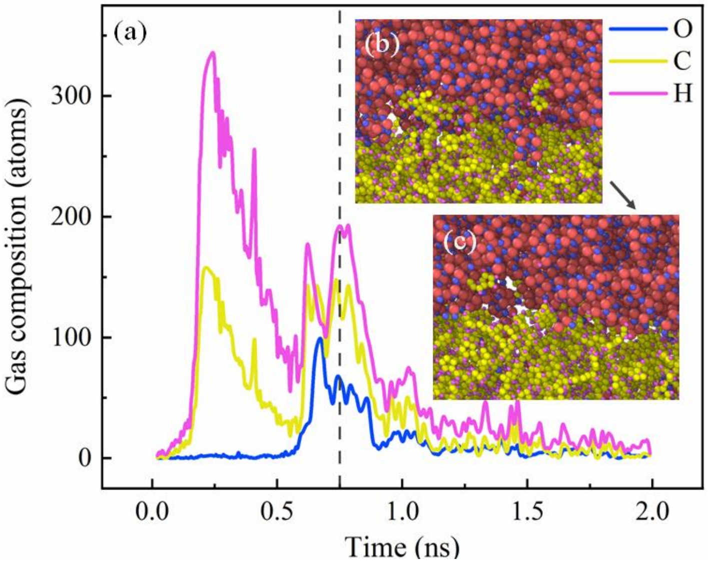

Fig. 3. (a) Gas loss over time; two consecutive atomic structures of a simulated region at 0.75 ns (b) and 0.7505 ns (c). In both images, the color scheme is as follows: Si-red, O-blue, C-yellow, H-pink.

4. Conclusions

In this work, carbothermal reduction of SiO_2 in PSO-derived SiOC ceramics was studied using ReaxFF simulation in LAMMPS with >93K atoms and up to ~6 ns simulation time. We demonstrate for the first time that SiOC evolves into different clusters during pyrolysis along with compositional changes, especially O loss. Also, SiO_2 cluster size plays an important role in the diffusion of C into SiO_2 clusters. Only larger SiO_2 clusters are capable of O reduction while smaller SiO_2 regions cannot accommodate C diffusion. C cluster growth is correlated with O removal. C diffusion into SiO_2 cluster further confirms that carbothermal reduction is dependent on SiO_2

cluster size. This is the first report on the O removal and C interaction with different SiO_2 clusters in polymer derived SiOC systems.

Author Contributions:

The manuscript was written through contributions of all authors. / All authors have given approval to the final version of the manuscript. / C. Chaney's contributions are conceptualization, data curation, formal analysis, investigation, methodology, software, validation, visualization, writing-original draft, writing-review & editing. K. Lu's contributions are conceptualization, formal analysis, funding acquisition, investigation, methodology, project administration, resources, supervision, validation, visualization, writing-original draft, writing-review & editing.

Funding Sources:

The authors would like to acknowledge the financial support from National Science Foundation under Grant No. CBET-2024546 and Air Force Office of Scientific Research under grant number FA9550-22-1-0081.

Competing Interests:

The authors declare that they have no known competing financial interests or non-financial interests that could have appeared to influence the work reported in this paper.

Data Availability:

The data required to reproduce these findings are available from https://data.lib.vt.edu.

References:

[1] N. Grassie, I.G. Macfarlane, K.F. Francey, The thermal degradation of polysiloxanes—II. Poly(methylphenylsiloxane), European Polymer Journal, 15 (1979) 415-422.

[2] N. Grassie, I.G. Macfarlane, The thermal degradation of polysiloxanes—I. Poly(dimethylsiloxane), European Polymer Journal, 14 (1978) 875-884.

[3] K. Lu, D. Erb, Polymer derived silicon oxycarbide-based coatings, International Materials Reviews, 63 (2018) 139-161.

[4] R. Ma, K. Lu, D. Erb, Effect of solvent in preparation of SiOC bulk ceramics, Materials Chemistry and Physics, 218 (2018) 140-146.

[5] D. Erb, K. Lu, Effect of additive structure and size on SiO_2 formation in polymer-derived SiOC ceramics, Journal of the American Ceramic Society, 101 (2018) 5378-5388.

[6] Q. Wen, Z. Yu, R. Riedel, The fate and role of in situ formed carbon in polymer-derived ceramics, Progress in Materials Science, 109 (2020) 100623.

[7] A.W. Weimer, K.J. Nilsen, G.A. Cochran, R.P. Roach, Kinetics of carbothermal reduction synthesis of beta silicon carbide, AIChE Journal, 39 (1993) 493-503.

[8] A.V. Rau, K. Knott, K. Lu, Porous SiOC/SiC ceramics via an active-filler-catalyzed polymer-derived method, Materials Chemistry Frontiers, 5 (2021) 6530-6545.

[9] L. Wang, K. Lu, R. Ma, Effects of different polymer precursors on the characteristics of SiOC bulk ceramics, Applied Physics A, 125 (2019).

[10] P. Colombo, G. Mera, R. Riedel, G.D. Sorarù, Polymer-derived ceramics: 40 years of research and innovation in advanced ceramics, Journal of the American Ceramic Society, (2010) 1805–1837.

[11] D. Erb, K. Lu, Effects of SiO_2-forming additive on polysiloxane derived SiOC ceramics, Microporous and Mesoporous Materials, 266 (2018) 75-82.

[12] D. Erb, K. Lu, Effect of additive structure and size on SiO_2 formation in polymer-derived SiOC ceramics, Journal of the American Ceramic Society, 101 (2018) 5378-5388.

[13] J.K. Li, K. Lu, T.S. Lin, F.Y. Shen, Preparation of micro-/mesoporous SiOC bulk ceramics, Journal of the American Ceramic Society, 98 (2015) 1753-1761.

[14] K. Lu, Porous and high surface area silicon oxycarbide-based materials-A review, Materials Science and Engineering R, 97 (2015) 23-49.

[15] S. Naserifar, L. Liu, W.A. Goddard, T.T. Tsotsis, M. Sahimi, Toward a process-based molecular model of SiC membranes. 1. Development of a Reactive Force Field, The Journal of Physical Chemistry C, 117 (2013) 3308-3319.

[16] K. Chenoweth, S. Cheung, A.C.T. Van Duin, W.A. Goddard, E.M. Kober, Simulations on the thermal decomposition of a poly(dimethylsiloxane) polymer using the ReaxFF Reactive Force Field, Journal of the American Chemical Society, 127 (2005) 7192-7202.

[17] H.F. Gao, H.J. Wang, Z.H. Zhao, M. Niu, L. Su, Y. Wei, Reactive dynamics simulation study on the pyrolysis of polymer precursors to generate amorphous silicon oxycarbide structures, Journal of Physical Chemistry C, 122 (2018) 5767-5773.

[18] I. Ponomarev, A.C.T. van Duin, P. Kroll, Reactive Force Field for simulations of the pyrolysis of polysiloxanes into silicon oxycarbide ceramics, The Journal of Physical Chemistry C, 123 (2019) 16804-16812.

[19] R. Montgomery-Walsh, S. Nimbalkar, J. Bunnell, S.L. Galindo, S. Kassegne, Molecular dynamics simulation of evolution of nanostructures and functional groups in glassy carbon under pyrolysis, Carbon, 184 (2021) 627-640.

[20] C. Ma, Y. Li, Phase transition in polymer derived ceramics (PDCs) and its effect on mechanical response, International Journal of Computational Materials Science and Engineering, 12 (2021) 1962-1972.

[21] A.P. Thompson, H.M. Aktulga, R. Berger, D.S. Bolintineanu, W.M. Brown, P.S. Crozier, P.J. in 't Veld, A. Kohlmeyer, S.G. Moore, T.D. Nguyen, R. Shan, M.J. Stevens, J. Tranchida, C. Trott, S.J. Plimpton, LAMMPS - a flexible simulation tool for particle-based materials modeling at the atomic, meso, and continuum scales, Computer Physics Communications, 271 (2022) 108171.

[22] A.C.T. van Duin, S. Dasgupta, F. Lorant, W.A. Goddard, ReaxFF: A Reactive Force Field for hydrocarbons, The Journal of Physical Chemistry A, 105 (2001) 9396-9409.

[23] H.M. Aktulga, J.C. Fogarty, S.A. Pandit, A.Y. Grama, Parallel reactive molecular dynamics: Numerical methods and algorithmic techniques, Parallel Computing, 38 (2012) 245-259.

[24] N. Keller, O. Reiff, V. Keller, M.J. Ledoux, High surface area submicrometer-sized beta-SiC particles grown by shape memory synthesis method, Diamond & Related Materials, 14 (2005) 1353-1360.

[25] H. Preiss, L.M. Berger, M. Braun, Formation of black glasses and silicon carbide from binary carbonaceous/silica hydrogels, Carbon, 33 (1995) 1739-1746.

[26] M. Sharma, R.K. Upadhyay, S.S. Amritphale, N. Chandra, Synthesis of nano-structured 3C-SiC by carbothermal reduction of silicon bearing gel and carbon soot, Materials Letters, 65 (2011) 2161-2164.

[27] A.W. Weimer, K.J. Nilsen, G.A. Cochran, R.P. Roach, Kinetics of carbothermal reduction synthesis of beta silicon-carbide, AIChE Journal, 39 (1993) 493-503.

[28] Y. Hwang, D.H. Riu, H.J. Kang, J.H. An, W.S. Jung, D. Chun, Y. Kim, Carbothermal synthesis of beta-SiC powders from silicon and SiO_2-coated carbon powders, International Journal of Materials Research, 105 (2014) 392-396.

[28] K. Wang, H.T. Wang, Y.B. Cheng, Synthesis of nanostructured silicon carbide spheres from mesoporous C-SiO_2 nanocomposites, Chemical Communications, 46 (2010) 303-305.

[30] J.K. Li, K. Lu, Highly porous SiOC bulk ceramics with water vapor assisted pyrolysis, Journal of the American Ceramic Society, 98 (2015) 2357-2365.

[31] J. Latournerie, P. Dempsey, D. Hourlier-Bahloul, J.-P. Bonnet, Silicon oxycarbide glasses: Part 1—Thermochemical stability, Journal of the American Ceramic Society, 89 (2006) 1485-1491.

[32] G. Gregori, H.-J. Kleebe, D.W. Readey, G.D. Soraru̇, Energy-filtered TEM study of Ostwald ripening of Si nanocrystals in a SiOC glass, Journal of the American Ceramic Society, 89 (2006) 1699-1703.

[33] S. Yu, R. Tu, T. Goto, Preparation of SiOC nanocomposite films by laser chemical vapor deposition, Journal of the European Ceramic Society, 36 (2016) 403-409.

[34] L. Wang, K. Lu, R. Ma, Effects of different polymer precursors on the characteristics of SiOC bulk ceramics, Applied Physics A, 125 (2019) 395.

[35] L. Wang, K. Lu, Phase development of silicon oxycarbide nanocomposites during flash pyrolysis, Journal of Materials Science, 54 (2019) 6073-6087.

[36] S. Cetinkaya, S. Eroglu, Chemical vapor deposition of C on SiO_2 and subsequent carbothermal reduction for the synthesis of nanocrystalline SiC particles/whiskers, International Journal of Refractory Metals and Hard Materials, 29 (2011) 566-572.

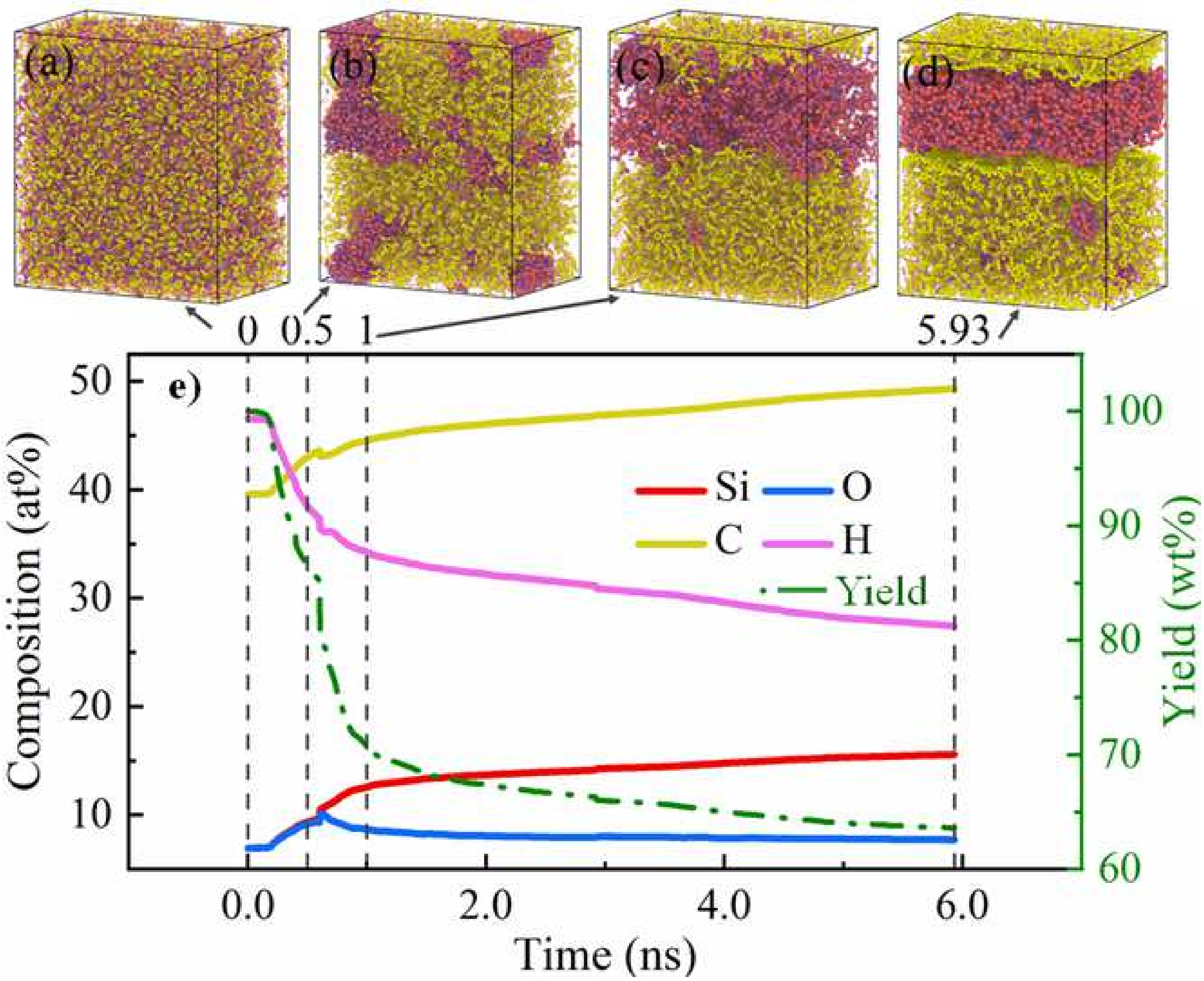
(a)
(b)
(c)
(d)
0
0.5
1
5.93
e)
Si
O
C
H
Yield
Composition (at%)
Yield (wt%)
Time (ns)
50
40
30
20
10
100
90
80
70
60
0.0
2.0
4.0
6.0

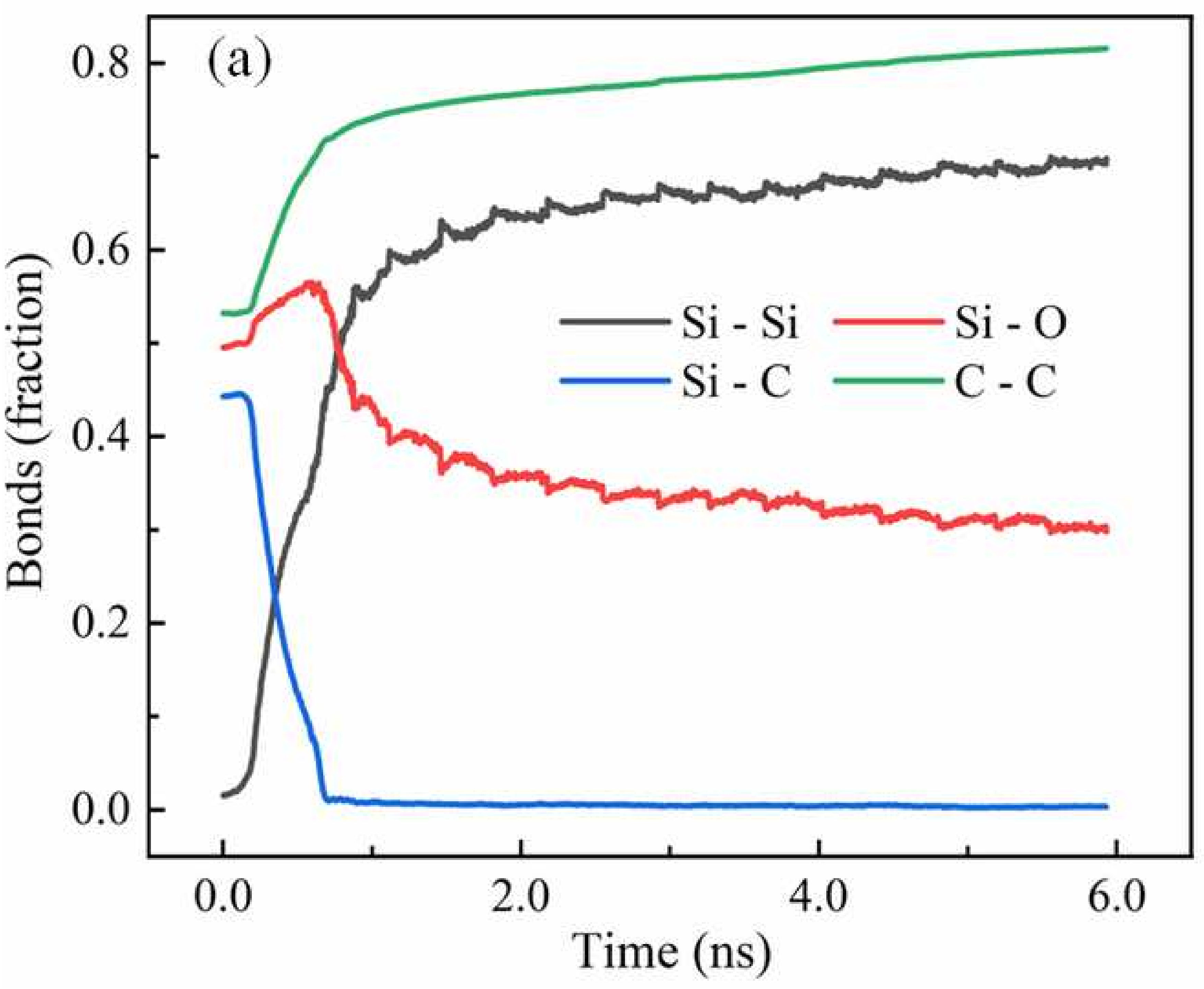
(a)
0.8
0.6
0.4
0.2
0.0
Bonds (fraction)
0.0
2.0
4.0
6.0
Time (ns)
Si - Si
Si - O
Si - C
C - C

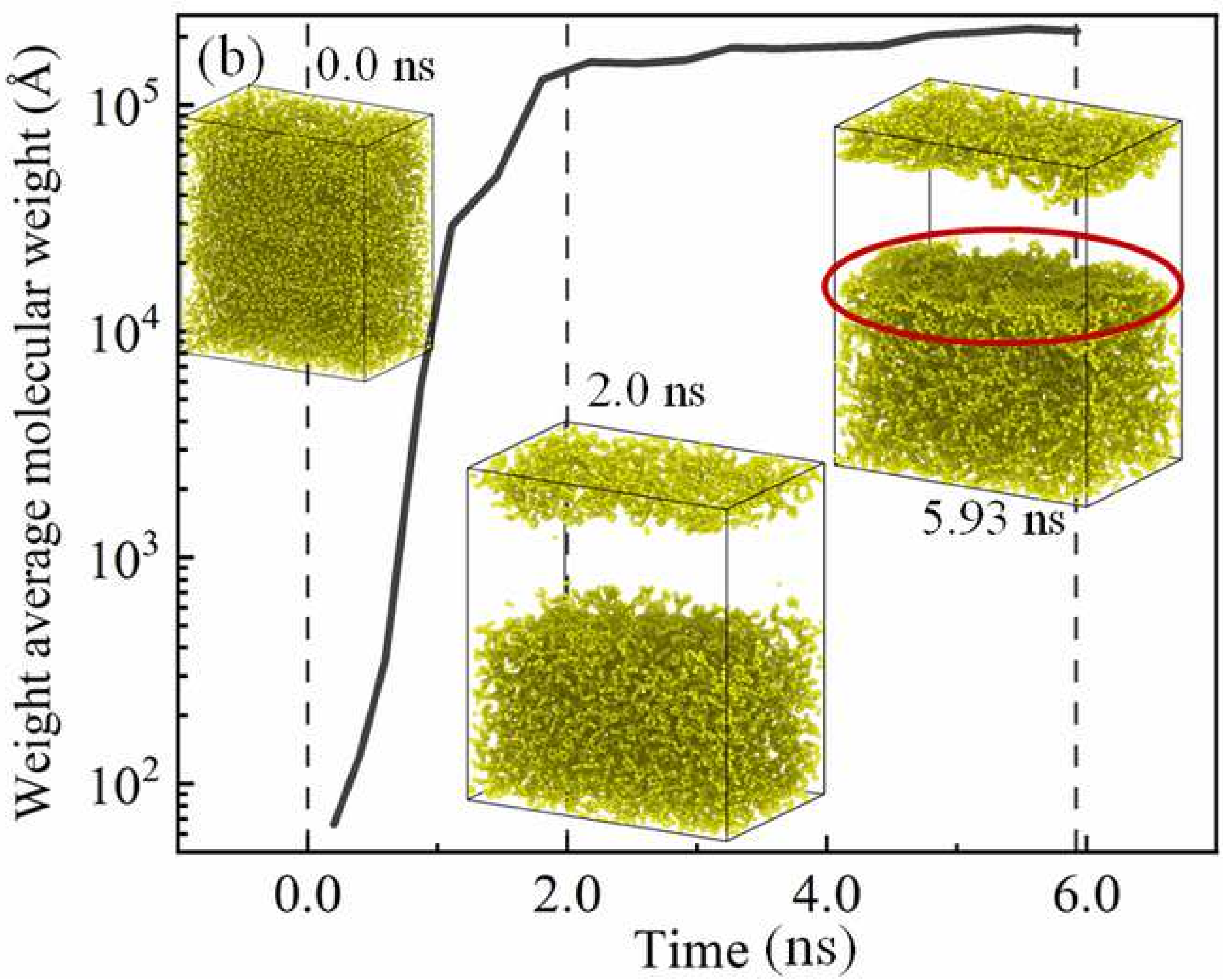
(b)
0.0 ns
2.0 ns
5.93 ns
Weight average molecular weight (Å)
10^5
10^4
10^3
10^2
0.0
2.0
4.0
6.0
Time (ns)

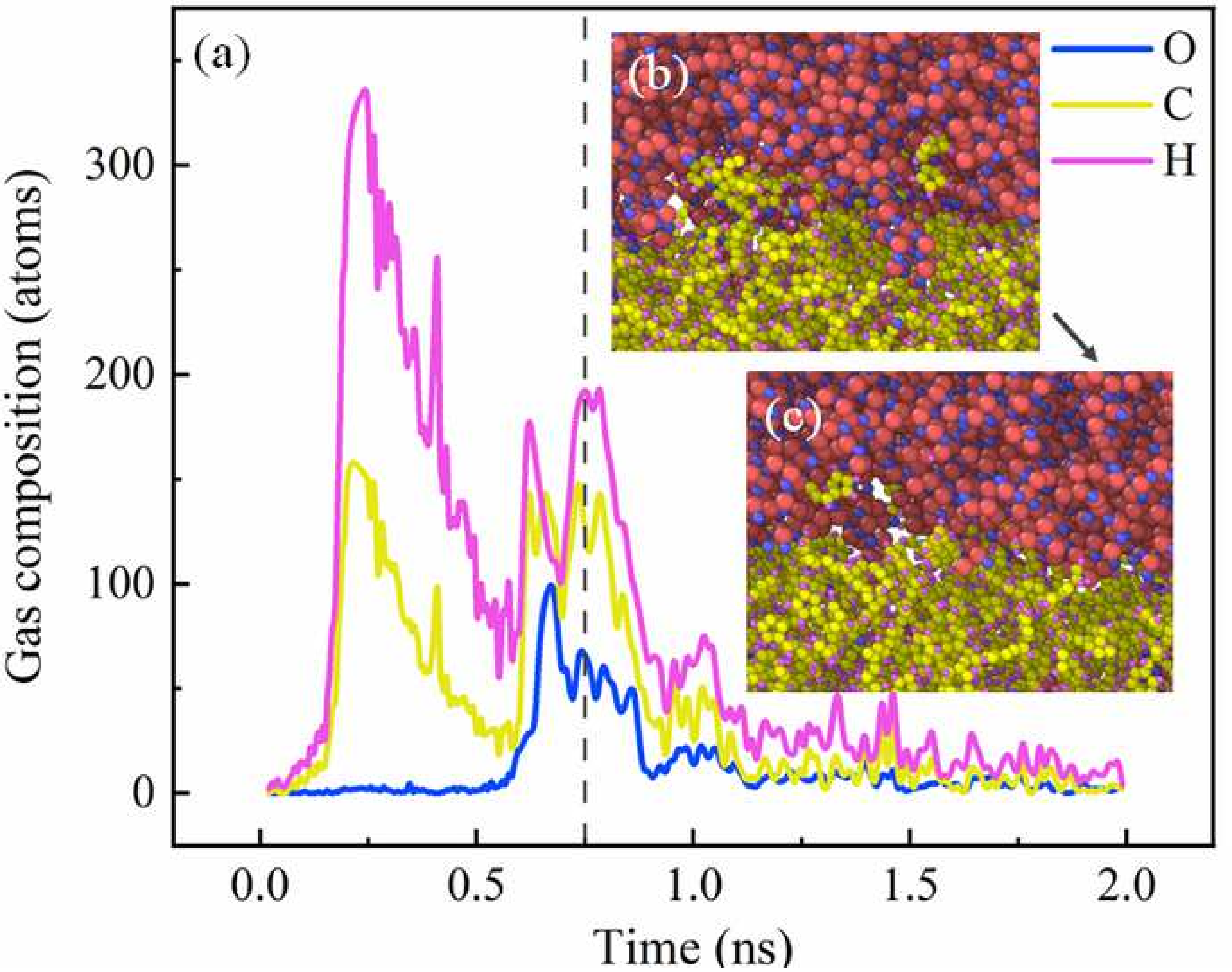
(a)
(b)
(c)
O
C
H
Gas composition (atoms)
0
100
200
300
0.0
0.5
1.0
1.5
2.0
Time (ns)